Ti/Al/Ti/Ni/Au ohmic contacts on AlGaN/GaN high electron mobility transistors with improved surface morphology and low contact resistance

Yu-Sheng Chiu, Tai-Ming Lin, Hong-Quan Nguyen, Yu-Chen Weng, Chi-Lang Nguyen, Yueh-Chin Lin, Hung-Wei Yu, Edward Yi Chang, and Ching-Ting Lee

Citation: Journal of Vacuum Science & Technology B **32**, 011216 (2014); doi: 10.1116/1.4862165

View online: http://dx.doi.org/10.1116/1.4862165

View Table of Contents: http://scitation.aip.org/content/avs/journal/jvstb/32/1?ver=pdfcov

Published by the AVS: Science & Technology of Materials, Interfaces, and Processing

Articles you may be interested in

Microstructure of Ti/Al/Ni/Au ohmic contacts for N-polar GaN/AlGaN high electron mobility transistor devices
J. Vac. Sci. Technol. B **32**, 011201 (2014); 10.1116/1.4829878

Analysis of surface roughness in Ti/Al/Ni/Au Ohmic contact to AlGaN/GaN high electron mobility transistors
Appl. Phys. Lett. **97**, 062115 (2010); 10.1063/1.3479928

Annealing temperature stability of Ir and Ni-based Ohmic contacts on Al Ga N Ga N high electron mobility transistors
J. Vac. Sci. Technol. B **22**, 2635 (2004); 10.1116/1.1814111

Metal/Al-doped ZnO ohmic contact for AlGaN/GaN high electron mobility transistor
Appl. Phys. Lett. **84**, 3996 (2004); 10.1063/1.1738175

Comparison of Ir and Ni-based Ohmic contacts for AlGaN/GaN high electron mobility transistors
J. Vac. Sci. Technol. B **22**, 619 (2004); 10.1116/1.1667508

Re-register for Table of Content Alerts

Create a profile.
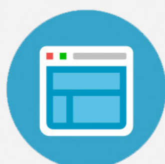
Sign up today!
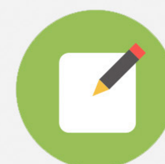

Redistribution subject to AVS license or copyright; see http://scitation.aip.org/termsconditions. Download to IP: 140.113.38.11 On: Fri, 02 May 2014 03:58:53

Ti/Al/Ti/Ni/Au ohmic contacts on AlGaN/GaN high electron mobility transistors with improved surface morphology and low contact resistance

Yu-Sheng Chiu,[a] Tai-Ming Lin,[a] and Hong-Quan Nguyen
Department of Materials Science and Engineering, National Chiao Tung University, 1001 Ta-Hsueh Rd., Hsinchu 300, Taiwan

Yu-Chen Weng
Institute of Lighting and Energy Photonics, College of Photonics, National Chiao Tung University, Tainan 71150, Taiwan

Chi-Lang Nguyen, Yueh-Chin Lin, Hung-Wei Yu, and Edward Yi Chang[b]
Department of Materials Science and Engineering, National Chiao Tung University, 1001 Ta-Hsueh Rd., Hsinchu 300, Taiwan

Ching-Ting Lee
Department of Electrical Engineering, National Cheng-Kung University, 1, University Road, Tainan 701, Taiwan

(Received 31 July 2013; accepted 27 December 2013; published 16 January 2014)

Optimizing surface morphology of ohmic contacts on GaN high electron mobility transistors continues to be a challenge in the GaN electronics industry. In this study, a variety of metal schemes were tested under various annealing conditions to obtain contacts with optimal qualities. A Ti/Al/Ti/Ni/Au (20/120/40/60/50 nm) metal scheme demonstrated the lowest contact resistance (R_c) and a smooth surface morphology, and the mechanisms were investigated by materials analysis. A Ti/Al/Ti/Ni/Au metal scheme with optimized Ti and Ni thicknesses can result in formation of a larger proportion of Al-Ni intermetallics and a continuous TiN interlayer, which results in smooth surface and low R_c. © *2014 American Vacuum Society*. [http://dx.doi.org/10.1116/1.4862165]

I. INTRODUCTION

AlGaN/GaN high electron mobility transistors (HEMTs) exhibit excellent device performance because of their inherent material properties. Ohmic contacts on AlGaN/GaN HEMTs play an important role in the DC and RF performance of the devices by contributing to higher current density, lower on-resistance, and less resistive heating. In order to improve device performance, ohmic contacts should meet the requirements of low contact resistance (R_c), high thermal and electrical stability, and smooth surface morphology. Ohmic contacts with low R_c have been achieved by using Ti/Al-based metal schemes with high temperature rapid thermal annealing (RTA). Ti/Al/Ni/Au, Ti/Al/Mo/Au, and Ti/Al/Ti/Au metal schemes have been successful developed with low R_c.[1–3] The possible mechanisms ohmic contacts with low R_c involve the interfacial reaction of the Ti/Al bilayer with the AlGaN/GaN epitaxy structure. Three possible mechanisms—low Schottky barrier, tunneling, and spike formation—have been proposed based on the formation of nitrides (TiN, Ti_xAlN, or AlN) at the metal-GaN interface.[4–6] Experimental results suggest that spike formation and tunneling are the mechanisms that account for ohmic contacts with lower R_c.

Low contact resistance (R_c) ohmic contacts on AlGaN/GaN HEMTs usually exhibit unfavorable surface morphology, which affects the process yield of the devices. After high temperature annealing, interdiffusion of ohmic contact metals results in bumpy surfaces. Several mechanisms have been proposed to explain this phenomenon. For example, melting and balling up of Al during RTA results in the formation of Al-Au intermetallics, which have been viewed as causes of such problematic surface morphology. Although barrier layers such as Ni, Pt, Mo, and Ti have been applied in an attempt to block the diffusion of Al and Au, most have been found ineffective.[7,8] A possible mechanism for the rough surface morphology on a conventional Ti/Al/Ni/Au metal scheme has been proposed by Gong *et al.*[9] Nonuniform precipitation of AlNi in the AlAu matrix is believed to account for the formation of the excessively rough surface of ohmic contacts on AlGaN/GaN HEMTs.

Several approaches have been tried to improve surface morphology of ohmic contacts on AlGaN/GaN HEMTs. Using a Au-free metal scheme, Ti/Al/Cr/Mo/Au metal scheme, or metal schemes with a thicker Ni layer, researchers have demonstrated a high success rate of forming ohmic contacts on AlGaN/GaN HEMTs with smooth surface morphologies, even at high annealing temperatures.[10–12] The thicknesses of individual metal layers have significant influence on the interface reaction and surface morphology of the ohmic contacts on AlGaN/GaN HEMT.[13] For instance, the Ti/Al ratio and Ni/Au ratio have been shown to have influence on R_c and surface morphology.[12,13] Furthermore, the Ti/Al/Ti/Ni/Au metal scheme has been used to demonstrate more favorable ohmic behavior compared to a Ti/Al/Ni/Au metal scheme after insertion of a 10-nm Ti interlayer.[14] However, there has not been a detailed study of surface morphology and formation mechanism for the Ti/Al/Ti/Ni/Au metal scheme. In this work, various metal schemes based on

[a]Yu-Sheng Chiu and Tai-Ming Lin contributed equally to this work.
[b]Author to whom correspondence should be addressed; electronic mail: edc@mail.nctu.edu.tw

Redistribution subject to AVS license or copyright; see http://scitation.aip.org/termsconditions. Download to IP: 140.113.38.11 On: Fri, 02 May 2014 03:58:53

TABLE I. Metal schemes designed in this study (nm).

Ti	Al	Ti	Ni	Au
20	120	0	100	50
20	120	20	80	50
20	120	40	60	50
20	120	100	0	50

Ti, Al, Ni, and Au were designed and tested to achieve ohmic contacts with smooth surface morphology and low R_c. The metal schemes were also analyzed by atomic force microscope (AFM) and transmission electron microscopy (TEM) to determine a possible formation mechanism.

II. EXPERIMENTAL METHODS

Ohmic contacts were fabricated on an AlGaN/GaN HEMT epistructure grown on 6-in. Si (111) with an AlN nucleation layer, 3-μm GaN buffer layer, and 20-nm $Al_{0.25}Ga_{0.75}N$ barrier layer. The wafers were first cleaned in acetone (ACE) and isopropyl alcohol (IPA) for 5 min to remove organic contamination, and native oxides were removed after soaking in buffer oxide etchant (BOE) for 5 min. Mesa isolation was performed using a dry etch process by inductively coupled plasma (ICP) reactor with Cl_2 plasma in Ar ambient for 3 min and 20 s. Ohmic regions were then defined by a lithography process. Before metallization, the wafers were soaked in 10% HCl solution to remove native oxides. Then, metal schemes listed in Table I were deposited by e-gun evaporator. After lift-off of metals, the wafers were annealed (RTA) at different temperatures (800, 830, 850, 870, and 900 °C) for 35 s in N_2 ambient. A conventional Ti/Al/Ni/Au (20/120/25/100 nm) ohmic contact with a thinner barrier layer also was fabricated for comparison, and the R_c was measured to be 0.52 Ω mm on this wafer.[15]

R_c of different metal schemes were measured by transmission line method (TLM) with gap spacing of 3, 5, 10, 20, and 36 μm. Surface morphology was examined for a $10 \times 10\ \mu m^2$ area of each metal scheme by Veeco D-3100 AFM and the images of conventional Ti/Al/Ni/Au (20/120/25/100 nm), Ti/Al/Ni/Au (20/120/100/50 nm), and Ti/Al/Ti/Ni/Au (20/120/40/60/50 nm) metal schemes were composed from Nanoscope software. To investigate the mechanisms for surface morphology and R_c improvement, cross-section TEM images and scanning-mode TEM images (STEMs) were obtained by electron dispersive x-ray spectroscopy (EDS). Line-scans were analyzed by JEM-2100F FETEM for Ti/Al/Ni/Au (20/120/100/50 nm) and Ti/Al/Ti/Ni/Au (20/120/40/60/50 nm) metal schemes.

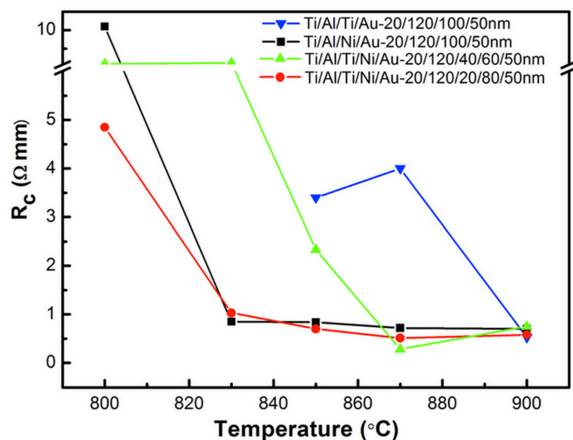

FIG. 1. (Color online) Contact resistance (R_c) of different metal schemes in Table I after annealing at various temperatures.

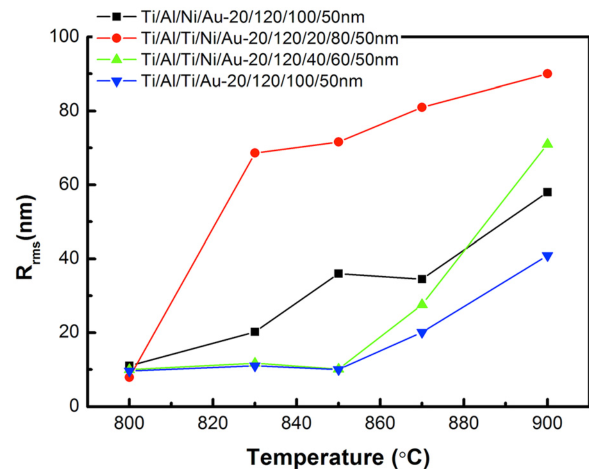

FIG. 2. (Color online) Surface roughness (R_{rms}) of different metal schemes in Table I after annealing at different temperatures.

III. RESULTS AND DISCUSSION

Contact resistances (R_c) for each metal scheme listed in Table I are measured. Figure 1 shows R_c values for the different metal schemes after annealing at various temperatures. Measurements showed that the Ti/Al/Ti/Au (20/120/100/50 nm) samples annealed at 800 and 830 °C exhibited Schottky behavior, so their R_c were not measurable. The

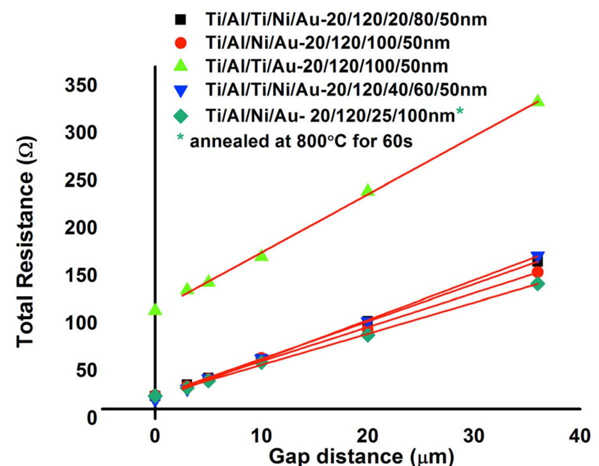

FIG. 3. (Color online) TLM measurement results for the different metal schemes annealed at 870 °C for 35 s and the conventional ohmic contact annealed at 800 °C for 60 s. Resistance at zero gap distance was derived by linear fitting.

Redistribution subject to AVS license or copyright; see http://scitation.aip.org/termsconditions. Download to IP: 140.113.38.11 On: Fri, 02 May 2014 03:58:53

lowest R_c for each metal scheme tended to decrease as the proportion of Ti interlayer increased. When the Ti/Ni barrier layer had a thickness of 40/60 nm, the lowest R_c value (0.28 Ω mm) was achieved, using the Ti/Al/Ti/Ni/Au (20/120/40/60/50 nm) annealed at 870 °C. For the other metal schemes, R_c values between 0.5 and 1 Ω mm were obtained following annealing at different temperatures. Surface roughness of each metal scheme after annealing at the various temperatures is shown in Fig. 2. As shown in Figs. 1 and 2, metal schemes with smoother surface morphology often resulted in higher R_c (>2 Ω mm). On the other hand, metal schemes with $R_c < 1$ Ω mm often resulted in rougher surface morphology. As stated above, Ti/Al/Ti/Ni/Au (20/120/40/60/50 nm) annealed at 870 °C for 35 s demonstrated the lowest R_c of the metal schemes in this study, and also showed improved surface morphology compared to conventional ohmic contacts. Although the Ti/Al/Ti/Au (20/120/100/50 nm) metal scheme also showed a low R_c (∼0.5 Ω mm) after annealing at 900 °C for 35 s, irregular patterns were found on the surface, as also observed by Mohammed *et al.*[8] To investigate the effects of Ti and Ni barrier layer thickness, the Ti/Al/Ti/Ni/Au (20/120/40/60/50 nm) and Ti/Al/Ni/Au (20/120/100/50 nm) samples annealed at 870 °C for 35 s samples were selected for further analysis. Figure 3 presents the TLM data for the different metal schemes annealed at 870 °C for 35 s, and the data for the conventional ohmic contact annealed at 800 °C for 60 s also is plotted for reference. Resistance at zero gap distance was derived by linear fitting of the other five points. The TLM data clearly demonstrate the excellent ohmic characteristic of the Ti/Al/Ti/Ni/Au (20/120/40/60/50 nm) scheme after annealing at 870 °C for 35 s.

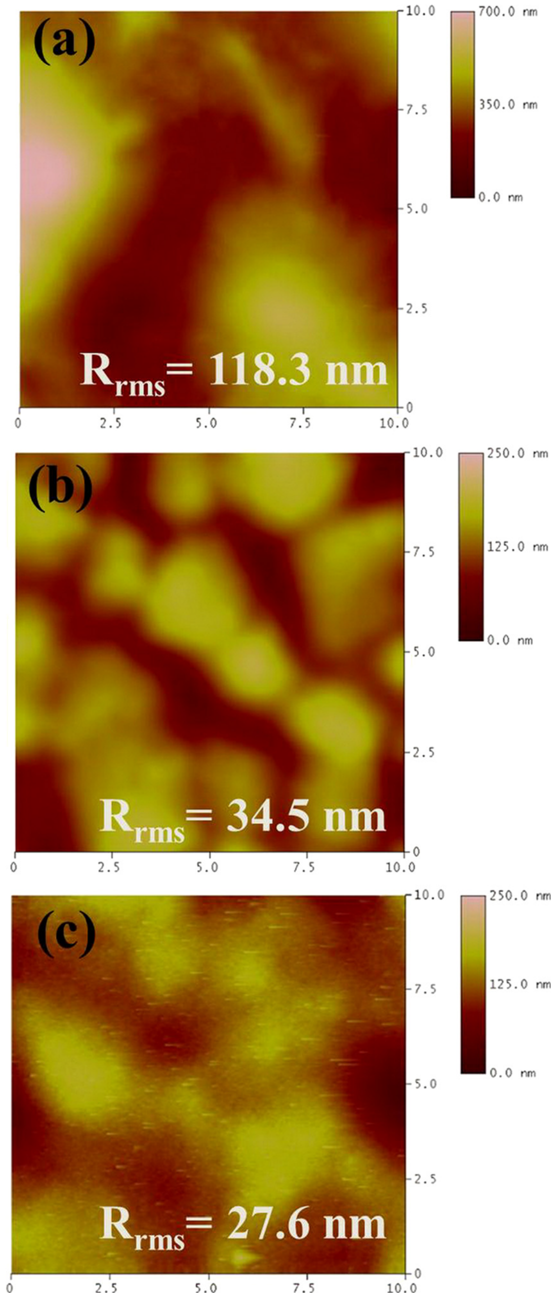

Fig. 4. (Color online) AFM scans of (a) conventional ohmic contact (Ti/Al/Ni/Au (20/120/25/100 nm), (b) Ti/Al/Ni/Au (20/120/100/50 nm), and (c) Ti/Al/Ti/Ni/Au (20/120/40/60/50 nm) metal schemes after RTA at 870 °C for 35 s. The R_{rms} values of images with scan size of 10×10 μm^2 are shown in the figures.

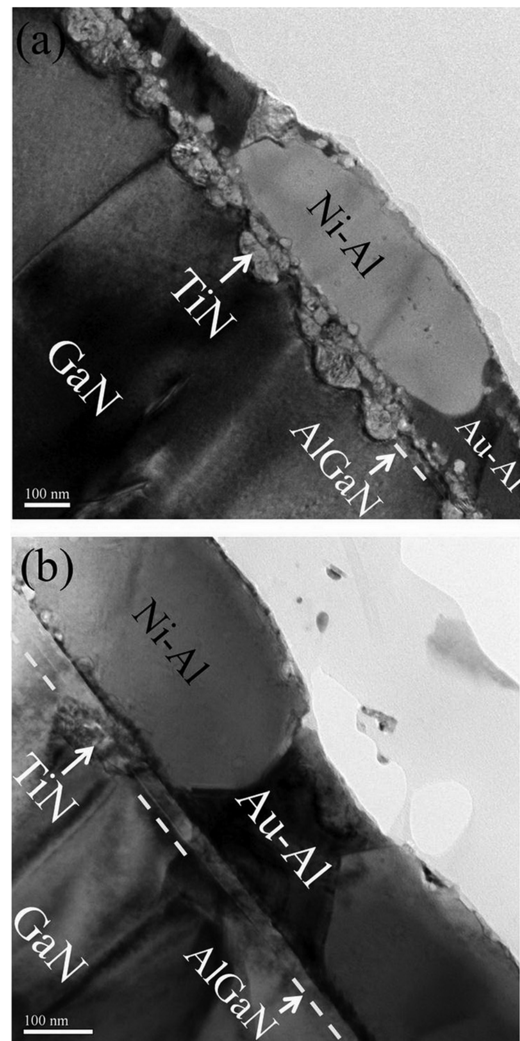

Fig. 5. Cross-section TEM images of (a) Ti/Al/Ti/Ni/Au (20/120/40/60/50 nm) and (b) Ti/Al/Ni/Au (20/120/100/50 nm) metal schemes after annealing at 870 °C for 35 s.

Redistribution subject to AVS license or copyright; see http://scitation.aip.org/termsconditions. Download to IP: 140.113.38.11 On: Fri, 02 May 2014 03:58:53

Figure 4 shows the comparison between the surface morphologies of the optimized Ti/Al/Ti/Ni/Au (20/120/40/60/50 nm), conventional Ti/Al/Ni/Au (20/120/25/100 nm), and Ti/Al/Ni/Au (20/120/100/50 nm) metal schemes. The conventional Ti/Al/Ni/Au ohmic contact has the roughest surface morphology with rms roughness (R_{rms}) of 118.3 nm, and the Ti/Al/Ti/Ni/Au (20/120/40/60/50 nm) metal scheme shows significant improvement in surface morphology with R_{rms} of 27.6 nm. The R_{rms} of Ti/Al/Ni/Au (20/120/100/50 nm) metal scheme was measured as 34.5 nm. In Fig. 4, it is evident that metal schemes with total barrier layer thicknesses of 100 nm are more likely to form ohmic contact with surfaces that are smoother than the conventional one, which has a barrier thickness of only 25 nm. A possible mechanism for these smoother surface morphologies on metal schemes with thicker barrier layers will be discussed in the following paragraphs.

TEM analysis of optimized Ti/Al/Ti/Ni/Au (20/120/40/60/50 nm) and Ti/Al/Ni/Au (20/120/100/50 nm) metal schemes are shown in Figs. 5 and 6. Figures 5(a) and 5(b) show the TEM cross-section images of the Ti/Al/Ti/

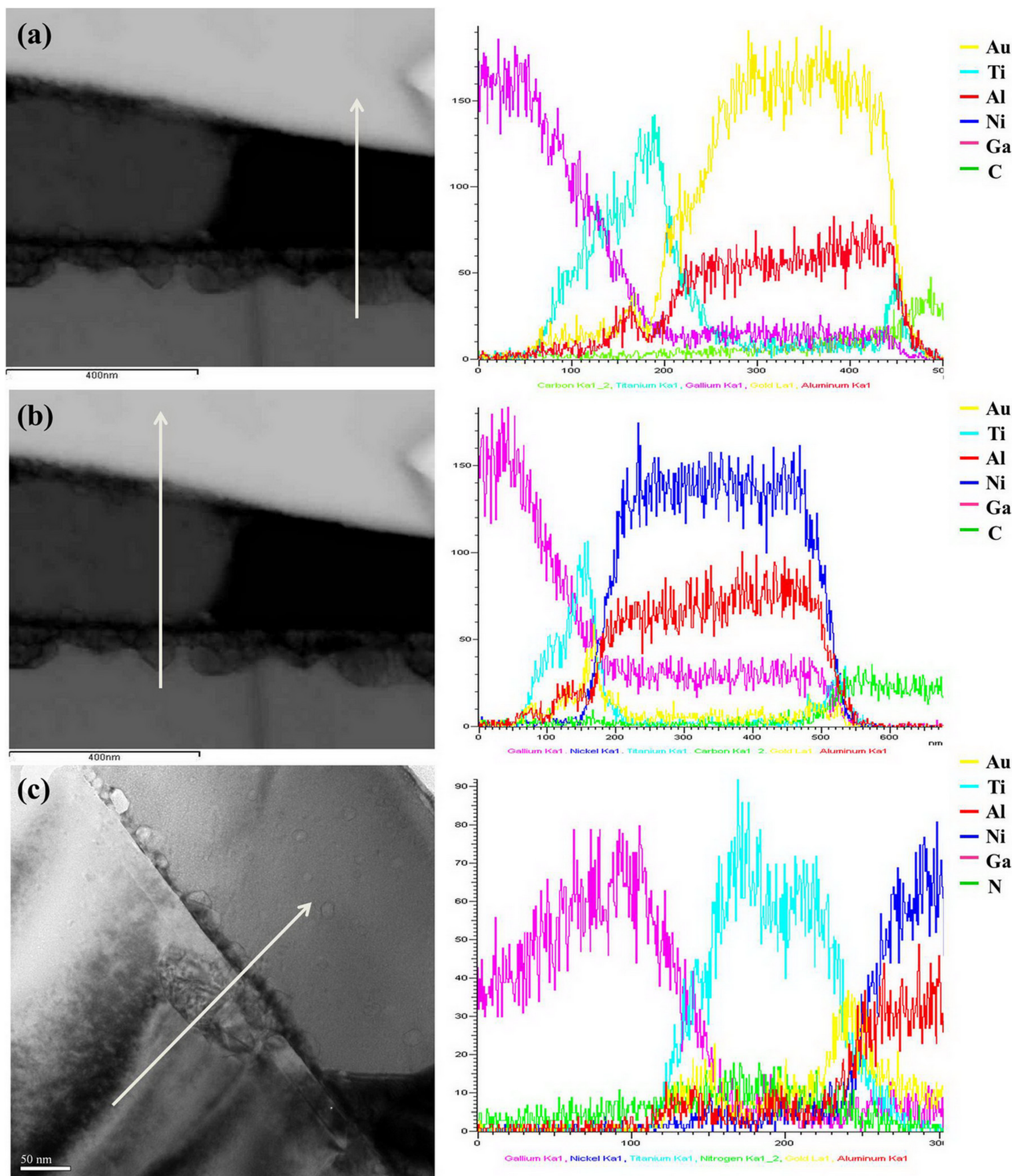

Fig. 6. (Color online) STEM images of (a) Ti/Al/Ti/Ni/Au (20/120/40/60/50 nm) metal scheme after RTA at 870 °C for 35 s with EDS line-scan result across the dark region on metal contact (as the arrow shows) and (b) Ti/Al/Ti/Ni/Au (20/120/40/60/50 nm) metal scheme after RTA at 870 °C for 35 s with EDS line-scan result across the bright region on metal contact (as the arrow shows). TEM image of (c) Ti/Al/Ni/Au (20/120/100/50 nm) metal scheme after RTA at 870 °C for 35 s and its corresponding EDS line-scan result (as the arrow shows).

Redistribution subject to AVS license or copyright; see http://scitation.aip.org/termsconditions. Download to IP: 140.113.38.11 On: Fri, 02 May 2014 03:58:53

Ni/Au (20/120/40/60/50 nm) and Ti/Al/Ni/Au (20/120/100/50 nm) samples, respectively. The EDS analysis results in Fig. 6 confirm that the bright grains are mainly composed of Al and Ni, and the dark regions are mainly composed of Al and Au. Ti and Au were detected at the metal–GaN interface in both metal schemes, so the TiN spikes surrounded by Au may form at the interface, as has been previously reported.[5,6] Based on the TEM analysis, it is likely that the bumpy areas in the AFM image are bright grains composed of Al and Ni not related to the study or other Ti, Al, Ni, and Au-based metal schemes. From Figs. 5(a) and 5(b), the main difference between Ti/Al/Ni/Au (20/120/100/50 nm) and Ti/Al/Ti/Ni/Au (20/120/40/60/50 nm) is the form of TiN at the interface. TiN spikes can be observed at the metal-GaN interface of both metal schemes. When these spikes form, they create a direct contact path to the 2DEG and are more effective at forming low-R_c ohmic contacts than the thin layered TiN.[6] However, there is another continuous TiN layer of ~20 nm thickness between metal contacts and the TiN spikes in the Ti/Al/Ti/Ni/Au (20/120/40/60/50 nm) metal scheme. Moreover, a higher Ni ratio in the Ti/Al/Ni/Au (20/120/100/50 nm) metal scheme facilitates the formation of Al-Ni grains, resulting in a higher density of bumps on the surface.

The TEM images in this study [Figs. 5(a) and 5(b)] show improvement in surface morphology compare with conventional Ti/Al/Ni/Au metal schemes reported before[1,6,9] although the so-called "barrier layer" disintegrates and reacts with Al regardless of the barrier layer thickness. Different forms of Al-Ni grain precipitates were found after annealing. While Ni composition increased, large-sized Al-Ni grains precipitated adjacent to Al-Au grains with similar size rather than precipitating randomly in the Al-Au matrix. As a consequence, bumps on the surfaces of ohmic contacts with higher Ni composition had more reproducible heights than the conventional ohmic contacts, as revealed in the AFM and cross-section TEM images [Figs. 4–5(b)].

Both Ti/Al/Ni/Au (20/120/100/50 nm) and Ti/Al/Ti/Ni/Au (20/120/40/60/50 nm) metal schemes demonstrated smoother surface morphology than conventional ohmic contacts, but the Ti/Al/Ni/Au (20/120/100/50 nm) metal scheme had a higher R_c than the Ti/Al/Ti/Ni/Au (20/120/40/60/50 nm). The different interface reactions observed in cross-section TEM images may account for the difference. As in the conventional Ti/Al/Ni/Au interface reaction, TiN spikes that are considered to make direct contact paths with 2DEG locally protrude through the AlGaN layer.[16] However, the Ti/Al/Ni/Au (20/120/100/50 nm) metal scheme exhibited a higher R_c than the conventional Ti/Al/Ni/Au ohmic contacts. This is attributed to the formation of a higher proportion of Al-Ni inter-metallics, which have been reported in a previous study[17] to be more electrically resistive than the Al-Au intermetallics after annealing in the Ti/Al/Ni/Au (20/120/100/50 nm) metal scheme.[17] In other words, a higher percentage of Al-Ni intermetallics forming after annealing can improve the contact's surface morphology, at the cost of raising the R_c. Although highly resistive Al-Ni intermetallics are bulk of the Ti/Al/Ti/Ni/Au (20/120/40/60/50 nm) metal scheme after annealing, the metal scheme still demonstrated excellent ohmic characteristics. This may be due to the interface reactions, which form a continuous TiN layer of ~20 nm thickness in addition to the TiN spikes. The formation of this thick and continuous TiN layer is related to the insertion of a 40-nm Ti interlayer that consumes the AlGaN layer, such that the formation of TiN is not limited to local protrusions but also forms a connecting stripe at the interface. Formation of this TiN layer possibly results in lower R_c than the Ti/Al/Ni/Au (20/120/100/50 nm) metal scheme because of higher concentration of nitrogen vacancies generated due to the consumption of the AlGaN layer and consequent facilitation of the tunneling mechanism. Moreover, with the Ti interlayer lying between the Al and Ni layers, a smaller proportion of Al-Ni intermetallics was observed in Ti/Al/Ti/Ni/Au (20/120/40/60/50 nm) than in Ti/Al/Ni/Au (20/120/100/50 nm). The Ti interlayer may be blocking interdiffusion between the Al and Ni layers in this case.

IV. CONCLUSIONS

In summary, the most promising metal scheme we tested was Ti/Al/Ti/Ni/Au (20/120/40/60/50 nm), for which we achieved a low R_c of 0.28 Ω mm with improved surface morphology (R_{rms} 27.6 nm) after annealing at 870 °C for 35 s. Metal schemes with thicker barrier layers effectively reduced surface roughness. Larger Al-Ni intermetallics were observed alongside Al-Au intermetallics after annealing instead of small Al-Ni precipitates randomly distributed in the matrix of the metal contact, which may contribute to smoother surfaces with lower R_c. However, as the proportion of the Ni layer increased, formation of excess Al-Ni intermetallics resulted in rougher surfaces and higher R_c. Consequently, it is necessary to optimize Ti and Ni layer thicknesses within the metal scheme to keep surface morphology smooth and reduce R_c, by controlling the proportion of more resistive Al-Ni intermetallics in the film and facilitating the tunneling mechanism through a thick nitride at the interface.

ACKNOWLEDGMENTS

This study was supported financially by the National Science Council, ROC (NSC-101-2911-I-009-507) and the Nano Facility Center of National Chiao Tung University.

[1]A. N. Bright, P. J. Thomas, M. Weyland, D. M. Tricker, and C. J. Humphreys, J. Appl. Phys. **89**, 3143 (2001).
[2]J. A. Bardwell, G. I. Sproule, Y. Liu, H. Tang, J. B. Webb, J. Fraser, and P. Marshall, J. Vac. Sci. Technol. B **20**, 1444 (2002).
[3]D. Selvanathan, F. M. Mohammed, A. Tesfayesus, and I. Adesida, J. Vac. Sci. Technol. B **22**, 2409 (2004).
[4]S. Ruvimov *et al.*, Appl. Phys. Lett. **69**, 1556 (1996).
[5]L. Wang, F. M. Mohammed, and I. Adesida, J. Appl. Phys. **103**, 093516 (2008).
[6]A. Fontserè *et al.*, Appl. Phys. Lett. **99**, 213504 (2011).
[7]F. M. Mohammed, L. Wang, I. Adesida, and E. Piner, J. Appl. Phys. **100**, 023708 (2006).
[8]F. M. Mohammed, L. Wang, H. Joon Koo, and I. Adesida, J. Appl. Phys. **101**, 033708 (2007).
[9]R. Gong, J. Wang, S. Liu, Z. Dong, M. Yu, C. P. Wen, Y. Cai, and B. Zhang, Appl. Phys. Lett. **97**, 062115 (2010).

Redistribution subject to AVS license or copyright; see http://scitation.aip.org/termsconditions. Download to IP: 140.113.38.11 On: Fri, 02 May 2014 03:58:53

[10]H. S. Lee, D. S. Lee, and T. Palacios, IEEE Electron. Device Lett. **32**, 623 (2011).
[11]Y. L. Lan, H. C. Lin, H. H. Liu, G. Y. Lee, F. Ren, S. J. Pearton, M. N. Chang, and J. I. Chyi, Appl. Phys. Lett. **94**, 243502 (2009).
[12]H. P. Xin *et al.*, in CS MANTECH Conference, Portland, Oregon, USA, 17 May 2010, pp.149–152.
[13]X. Kong, K. Wei, G. Liu, and X. Liu, J. Phys. D: Appl. Phys. **45**, 265101 (2012).
[14]T. G. Kim, Y. S. Lee, S. J. Kim, H. G. Choi, and C. K. Hahn, J. Korean Phys. Soc. **56**, 1287 (2010).
[15]C. T. Chang, H. T. Hsu, E. Y. Chang, C. I. Kuo, J. C. Huang, C. Y. Lu, and Y. Miyamoto, IEEE Electron. Device Lett. **31**, 105 (2010).
[16]L. Wang, F. M. Mohammed, and I. Adesida, J. Appl. Phys. **101**, 013702 (2007).
[17]F. Roccaforte, F. Iucolano, F. Giannazzo, A. Alberti, and V. Raineri, Appl. Phys. Lett. **89**, 022103 (2006).

Redistribution subject to AVS license or copyright; see http://scitation.aip.org/termsconditions. Download to IP: 140.113.38.11 On: Fri, 02 May 2014 03:58:53